Kufa Journal of Engineering
Vol. 10, No. 2, April 2019, P.P. 60-75
Received 30 January 2018, accepted 4 June 2018

NONLINEAR ANALYSIS OF REINFORCED CONCRETE CORBELS STRENGTHENED WITH CARBON FIBRE REINFORCED POLYMER STRIPS BY ANSYS

Muhammad Abed Attiya[1] and Anis A. Mohamad-Ali[2]

[1] Civil Engineering Department, College of Engineering, University of Kufa, Iraq.
Email: mohammedw.alfatlawi@uokufa.edu.iq

[2] Civil Engineering Department, College of Engineering, University of Basra, Iraq.
Email: dr.anismohamadali@gmail.com

http://dx.doi.org/10.30572/2018/kje/100205

ABSTRACT

This research is devoted to investigate the effect of Carbon Fibre Reinforced Polymer (CFRP) strips on the behaviour and load carrying capacity of the strengthened concrete corbels. Numerical investigation was carried out. The experimental program variables include location, direction, amount of CFRP strips, effect of shear span to effective depth (a/d) ratio on the behaviour of strengthened corbels. All corbels had the same dimensions and flexural reinforcement and they were without horizontal shear steel reinforcement. ANSYS V.11.0 software was utilized in this work. Solid65, Solid45, Link8 and shell41 elements were used to model concrete, steel bearing plates, steel flexural reinforcing bars, and CFRP strips respectively. Full bond was assumed between CFRP sheets and concrete interface. The full Newton-Raphson method is used as a nonlinear solution algorithm. The displacement criteria are used for convergence. The adopted finite element analysis showed good agreement with experimental results throughout the load-deflection history, the maximum difference in the ultimate load was less by10%. However, the finite element models show a slightly stiffer response.

KEYWORDS: Corbel, Carbon Fiber, Strengthened, Nonlinear Analysis, Finite Element Analysis.

1. INTRODUCTION

Corbels are short-haunched cantilevers that project from the inner face of columns or concrete walls to support heavy concentrated loads of precast beams, gantry girders, and other precast system loads. The ratio of shear span to depth is often less than 1.0. The nonlinear stress behaviour of the short member is thus affected by the shear deformation in the elastic range and consequently the shear strength of the section becomes an important parameter for design consideration (Mattock et al, 1976). Design of corbels should have a special attention, since the strength of a precast concrete structure is mainly governed by the strength of the connections rather than the members. Since a corbel forms the main part of the connection between a beam and a column, it should be made stronger than either the beam or the column (ACI 318-08).

This paper deals with the finite element analysis of reinforced concrete corbels strengthened with CFRP strips and subjected vertical loads. This research includes the analysis of corbels by using a powerful nonlinear finite element method package (ANSYS V. 11.0).

The accuracy of the finite element models is determined by ensuring that the ultimate load is reasonably predicted in comparison with the experimental results (Mohamad Ali and Attiya, 2012), and the load-deflection curves are close to the experimental curves as well as the crack patterns are similar to that achieved from experimental test.

2. NUMERICAL MODELING OF MATERIALS PROPERTIES

2.1. Modeling of Concrete

Reinforced concrete is one of the composite materials that have complex behaviour, especially after cracking. Concrete behaves as linear-elastic before cracking. A new behaviour occurs at the onset of cracking, the behaviour in a plain parallel to the crack, is different from that in a plain perpendicular to the cracking surface. The orthotropic behaviour of concrete in tension together with the nonlinear inelastic behaviour in compression complicates the modeling of this material in connection with the finite element analysis (Bangash, 1989).

Fig. 1 is adopted in the present study to represent the behaviour of concrete in compression.

2.2. Modeling of Steel

In developing a finite element model of reinforced concrete member, at least three alternative representations of the reinforcement have been used (Al-Shaarbaf, 1990).

Distributed representation: the steel is assumed to be distributed over the concrete element, with a particular orientation angle θ. A composite-reinforcement constitutive relation is used in this

case. To derive such a relation, perfect bond must be assumed to occur between the concrete and the steel.

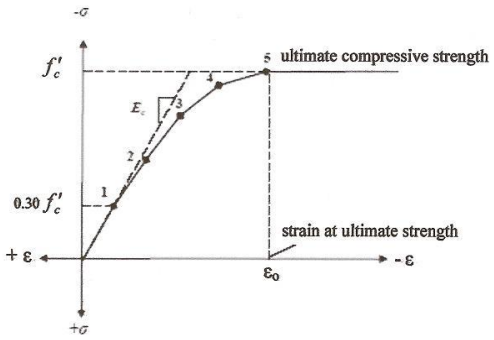

Fig. 1. Idealized uniaxial stress-strain curve for concrete (Willam and Warnke, 1975)

Embedded representation: the reinforcing bar is considered as an axial member built into the concrete element such that its displacements are consistent with that of the element. Also, perfect bond must be assumed to occur between the concrete and the steel.

Discrete representation: one-dimensional bar element may be used in this approach to simulate the reinforcement, this element is connected to concrete mesh nodes at bar location. Therefore, the concrete and the reinforcement mesh share the same nodes and concrete occupies the same regions occupied by the reinforcement. This representation is adopted in the present study.

In ANSYS computer program the behaviour of a steel bar is described by a bilinear stress-strain curve starting at the origin with positive stress and strain values. The initial slope of the curve is taken as the elastic modulus of the material. At the specified yield stress (fy=C1), the curve continues along the second slope defined by the tangent modulus C2 (having the same units as the elastic modulus). The tangent modulus cannot be less than zero nor greater than the elastic modulus. A typical uniaxial stress strain curve for a steel bar loaded in tension is shown in Fig. 2.

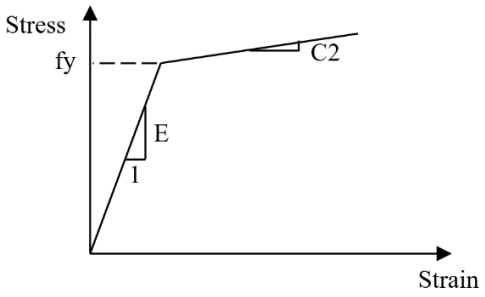

Fig. 2. Typical stress strain for steel bar (Al-Shaarbaf, 1990)

2.3. Modeling of CFRP Composites

FRP composites are materials that consist of two constituents. The constituents are combined at a macroscopic level and are not soluble in each other. One constituent is the reinforcement, which is embedded in the second constituent; a continuous polymer called the matrix. The reinforcing material is in the form of fibres, which are typically stiffer and stronger than the matrix. The FRP composites are anisotropic materials, that is, their properties are not the same in all directions.

Linear elastic orthotropic properties of the FRP composite are assumed thought out this study as shown in Fig. 3. In addition, full bond between the concrete and CFRPs is assumed.

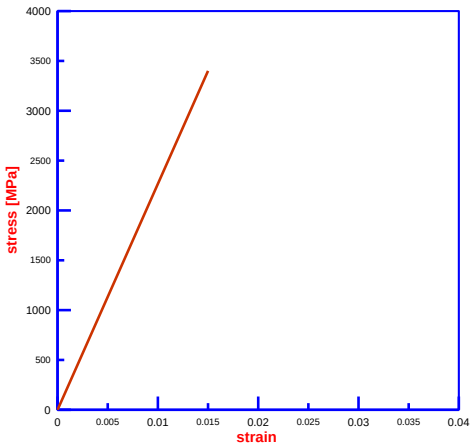

Fig. 3. Stress-strain relationship for FRP composite (Sika, 2005)

3. FINITE ELEMENT IDEALIZATION

In building a finite element model, it is necessary to define the element types, element real constants, material properties and the model geometry.

3.1. Element Types

The element types for this model are shown in Table 1. The SOLID65 element was used to model the concrete. Link180 was used to represent the main reinforcement and Shell41 represents the CFRP strips.

Table 1. Element types for working model

Material type	ANSYS element
Concrete	SOLID65
Steel plate	SOLID45
Reinforcement	LINKE8
CFRP strips	SHELL41

3.2. Modeling of the Structure

The dimensions and the reinforcement details for the corbels are presented in Fig. 4. By taking advantage of symmetry of the tested corbel, only one quarter of corbel was used for modeling as shown in Fig. 5. The overall mesh (for example CONT1) of the concrete, plate, and support volumes is shown in Fig. 6. For the other corbels, the same mesh of elements is used but the distribution of the elements in x and y-direction is modified to be more compatible with location of CFRP strips Fig. 7. The section below describes the mesh density, boundary condition and applying load techniques that adopted in the present study. A total of thirteen corbels were tested. The pertinent details are presented in Table 2. The three a/d ratios considered are 1.0, 0.7, and 0.5.

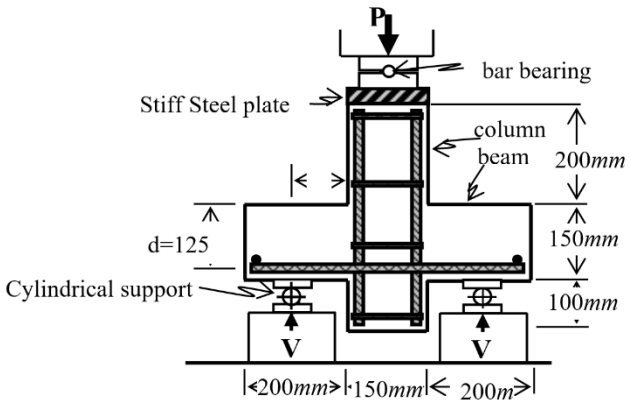

Fig. 4. Dimensions and reinforcement details (Mohamad Ali and Attiya, 2012).

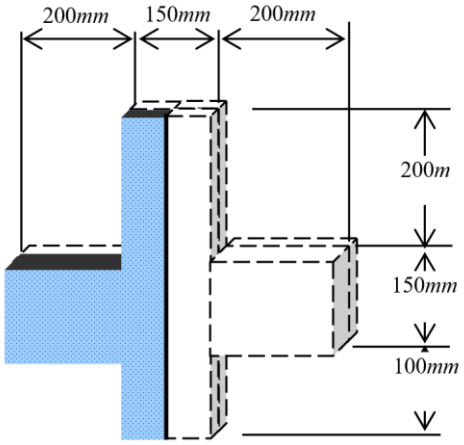

Fig. 5. Sketch for a quarter of the corbel model.

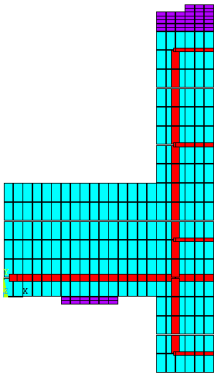

Fig. 6. Mesh of the concrete, steel plate, steel support and reinforcement configuration for corbels (control specimen without CFRP strip).

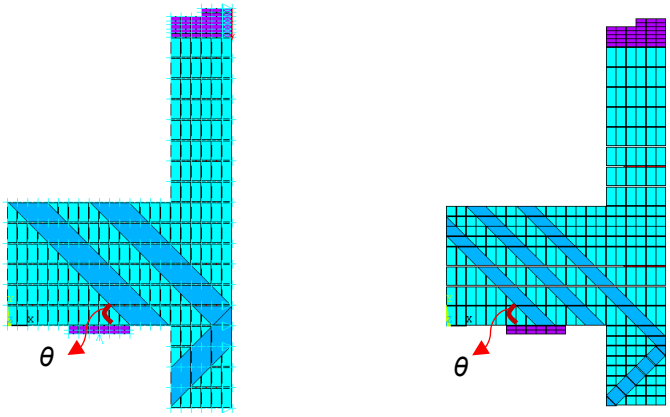

Fig. 7. Mesh for the quarter of corbel with inclined strengthening (CIS2 and CIS3).

Table 2. Details of the tested corbel.

Corbel designation	Strips inclination (θ)	Strips Thickness (*mm*)	Width of Strips (*mm*)	No. of Strips	(a/d) Ratio
CONT1	---	---	---	---	0.7
CIS2	45º	0.13	36.0	2	0.7
CIS3	45º	0.13	18.0	3	0.7
CIS4	45º	0.13	18.0	4	0.7
CISR2	45º	0.13	36.0	2	0.7
CISR3	45º	0.13	18.0	3	0.7
CISR4	45º	0.13	18.0	4	0.7
CISFR2	45º	0.13	36.0	2	0.7
CONT2	---	---	---	---	1.0
CISR2	45º	0.13	36.0	2	1.0
CONT3	---	---	---	---	0.5
CISR2	45º	0.13	36.0	2	0.5
CISR2	45º	0.13	36.0	2	0.7

3.3. Loading and Boundary Conditions

Displacement boundary conditions are needed to constrain the model to get unique representation for the actual corbel. Boundary condition need to apply at points of symmetry and where the supports and loads exist. The symmetry boundary conditions are set first. The model being used is symmetric about two planes. To model the symmetry, nodes on these planes must be constrained in the perpendicular directions. Therefore, the nodes in Ux and Uz have a degree of freedom equal to zero as shown in Fig. 8. The support (steel plate of 75x150x10) was modeled in such a way as a roller. A single line of nodes on the plate is given constraint in the UY direction. By doing this, the corbel will be allowed to rotate at the support,

as shown in Fig. 9. A steel plate of (75x150x10) and (150x150x25 mm) which is used at loading and reactions locations to avoid the situation of stress concentration. A line of load is applied to the center of steel plate at the location of the load, but due to symmetry the part of load which is lying on the symmetrical plane must be divided as illustrated in Fig. 10.

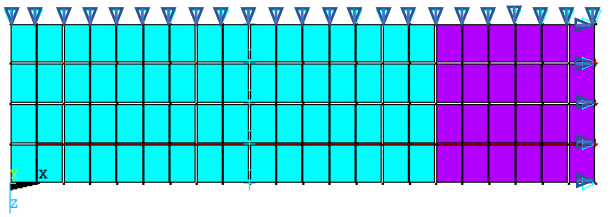

Fig. 8. Boundary conditions for planes of symmetry (top view).

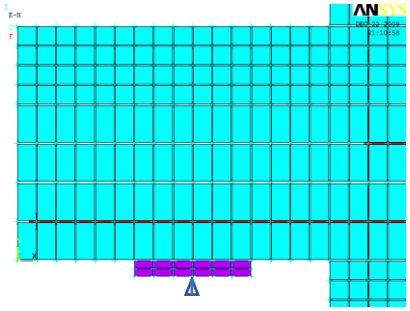

Fig. 9. Boundary conditions for support.

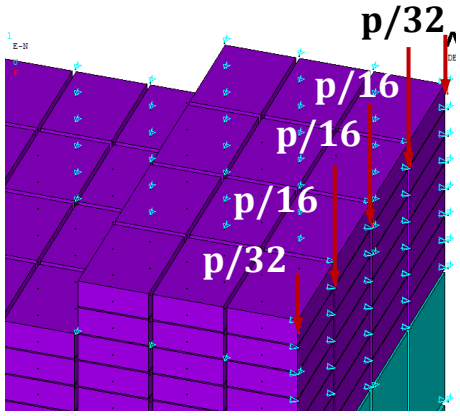

Fig. 10. Boundary conditions at the loading plates.

4. NUMERICAL RESULTS

To illustrate the validity of the proposed numerical method for the analysis of reinforced concrete corbels strengthened with CFRP strips, all tested corbels were analysed by using ANSYS computer program, as mentioned previously. The analysis follows the same procedure as that given in experimental work taking into account the variation in material properties, dimensions and other specifications.

4.1. Load Deflection Behaviour:

The experimental and numerical Load-deflection curves obtained for the tested corbels are shown in Figs. 11 - 21. In general, good agreement has been obtained by using the finite element model compared with the experimental results throughout the entire range of the behaviour. A

relatively stiffer numerical post-cracking response is noticed for all corbels as compared with the experimental results. Also, it can be seen that the axial ultimate load values obtained from the finite element analysis are slightly higher than the actual experimental ultimate loads.

The ratios of the predicted finite element ultimate loads to the corresponding experimental ultimate loads ranges between 0.991 and 1.098 of the analyzed corbels are listed in Table 3.

Table 3. A comparison between experimental and numerical ultimate loads of the analyzed corbels

Corbel designation	a/d	Numerical ultimate load (kN)	Experimental ultimate load (kN) (Mohamad Ali and Attiya,2012)	P_{nu}/P_{ex}
CONT1	0.7	314	292	1.075
CIS2	0.7	443	430	1.030
CIS3	0.7	443	422	1.049
CIS4	0.7	438	425	1.030
CISR2	0.7	509	467	1.089
CISR3	0.7	478	435	1.098
CISR4	0.7	488	447	1.091
CISFR4	0.7	473	454	1.041
CISR2 rep.	0.7	-	458	-
CONT2	1.0	233	235	0.991
CISR2	1.0	314	294	1.068
CONT3	0.5	389	358	1.086
CISR3	0.5	544	504	1.079

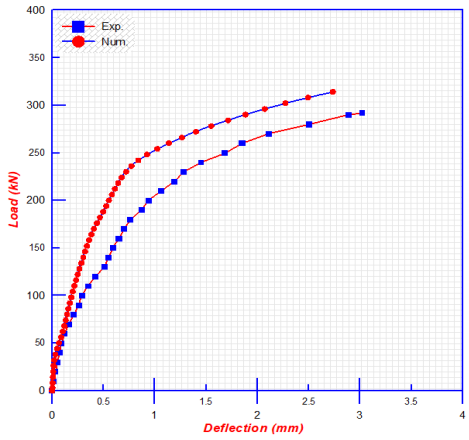

Fig. 11. Comparison between current numerical and experimental (Mohamad Ali and Attiya, 2012) load-deflection curve (CONT1).

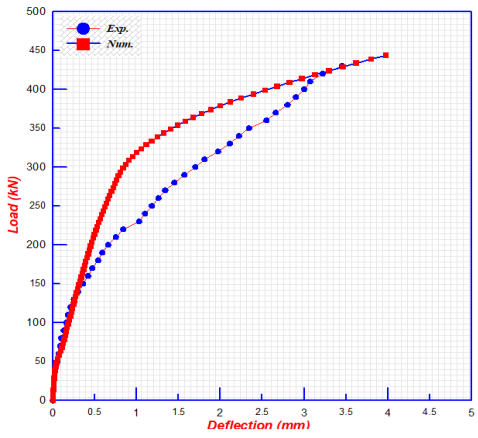

Fig. 12. Comparison between current numerical and experimental (Mohamad Ali and Attiya, 2012) load-deflection curve (CIS2)

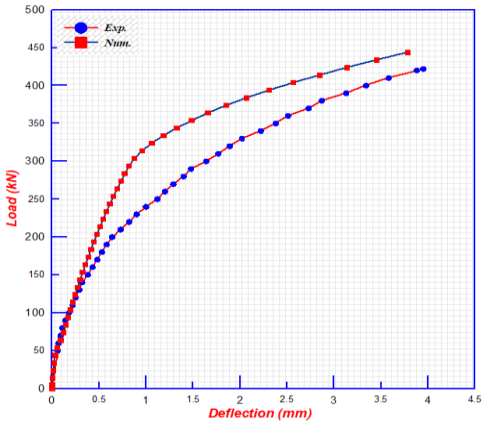

Fig. 13. Comparison between current numerical and experimental (Mohamad Ali and Attiya, 2012) load-deflection curve (CIS3).

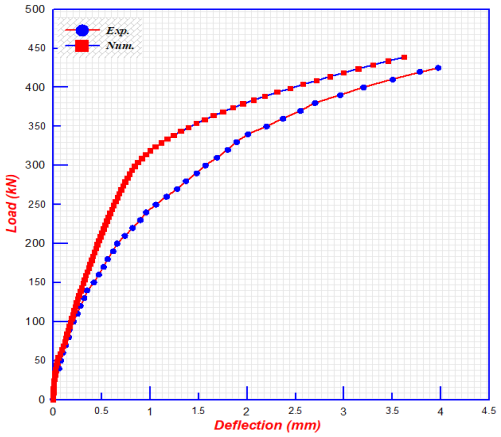

Fig. 14. Comparison between current numerical and experimental (Mohamad Ali and Attiya,2012) load-deflection curve (CIS4).

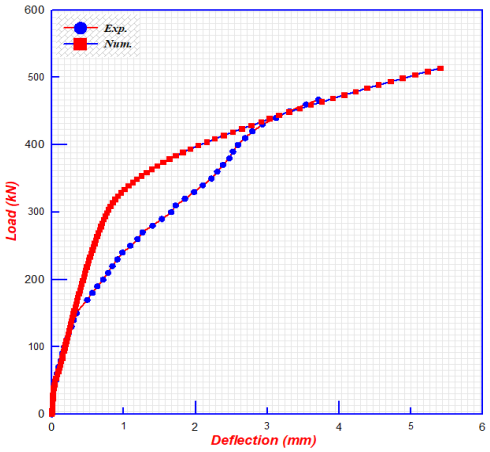

Fig. 15. Comparison between current numerical and experimental (Mohamad Ali and Attiya, 2012) load-deflection curve (CISR2).

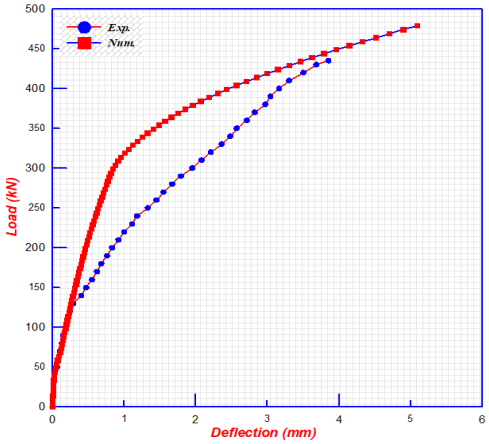

Fig. 16. Comparison between current numerical and experimental (Mohamad Ali and Attiya, 2012) load-deflection curve (CISR3)

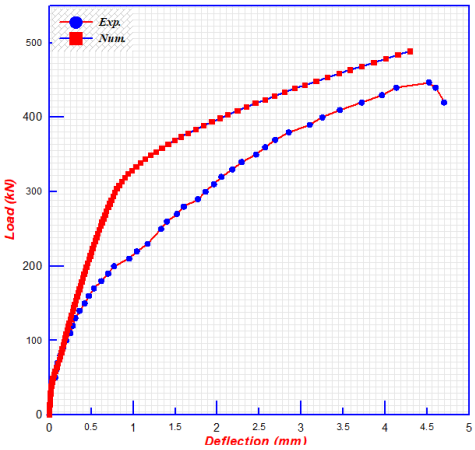

Fig. 17. Comparison between current numerical and experimental (Mohamad Ali and Attiya,2012) load-deflection curve (CISR4)

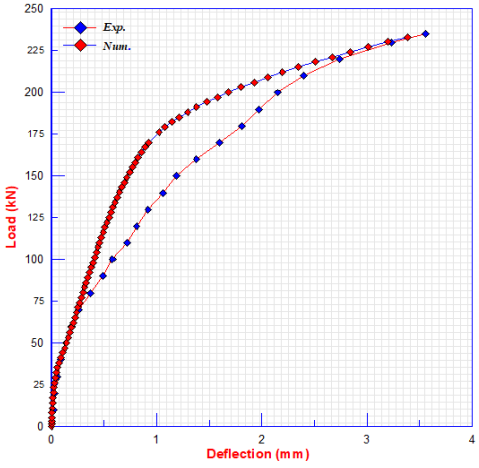

Fig. 18. Comparison between current numerical and experimental (Mohamad Ali and Attiya,2012) load-deflection curve (CONT2)

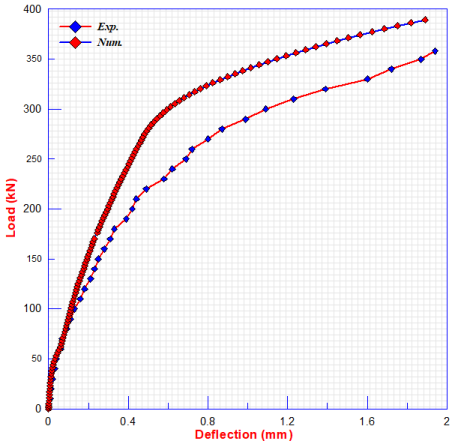

Fig. 19. Comparison between current numerical and experimental (Mohamad Ali and Attiya, 2012) load-deflection curve (CONT3).

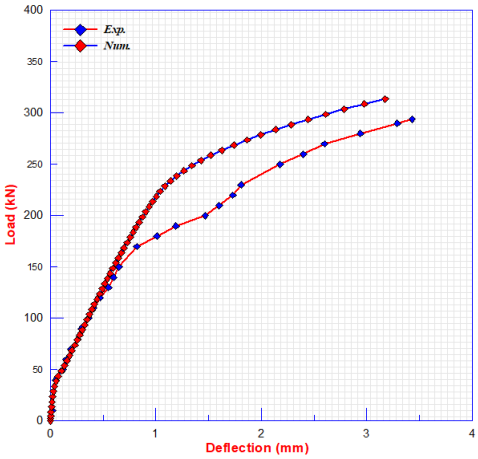

Fig. 20. Comparison between current numerical and experimental (Mohamad Ali and Attiya, 2012) load-deflection curve, a/d=1.0)

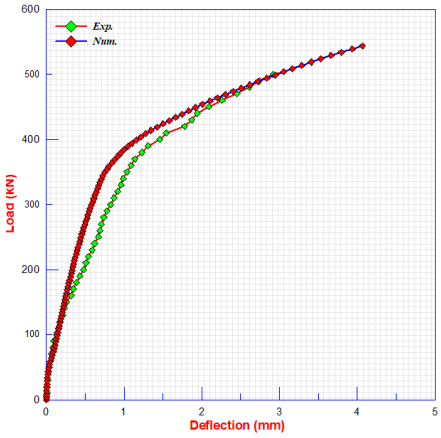

Fig. 21. Comparison between current numerical and experimental (Mohamad Ali and Attiya,2012) load-deflection curve, a/d=0.5).

4.2. Stress, Strain and Deflection Distribution

Specimen corbel CONT1, and CIS2 were taken for example to verify the application of the proposed numerical solution by using ANSYS computer program V11.0 software. The deflected shape of corbel CONT1, and CIS2 due to external applied loads and variation of stress in the longitudinal x, y, and x-y-direction, and variation of strain in x and y-direction is shown in Figs. 22 - 27. In these figures, it is obvious that the maximum stress is at upper of column face.

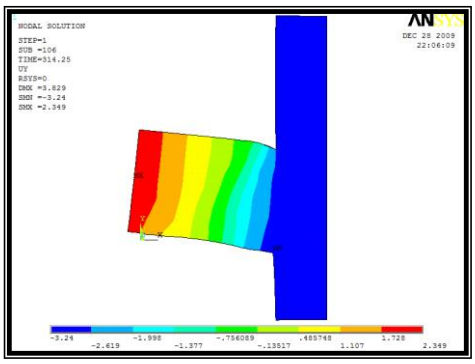

Fig. 22. Variation of deflection UY along quarter of corbel CONT1 at ultimate load.

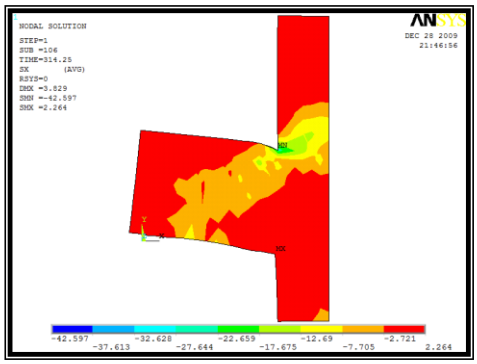

Fig. 23. Variation of stress in x-direction along quarter of concrete corbel CONT1 at ultimate load

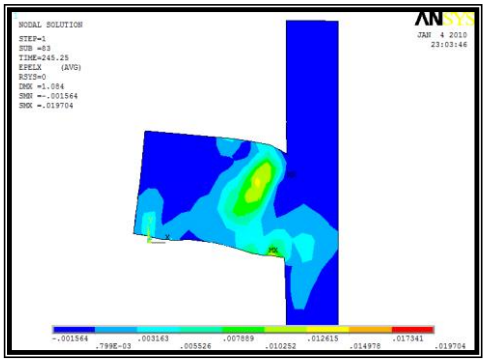

Fig. 24. Variation of strain in x-direction along quarter of concrete corbel CONT1 at ultimate load.

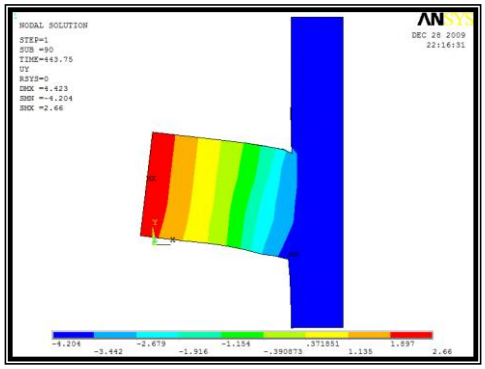

Fig. 25. Variation of deflection UY along quarter of corbel CIS2 at ultimate load.

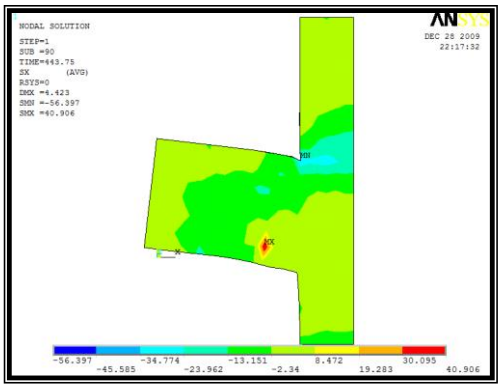

Fig. 26. Variation of stress in x-direction along quarter of concrete corbel CIS2 at ultimate load.

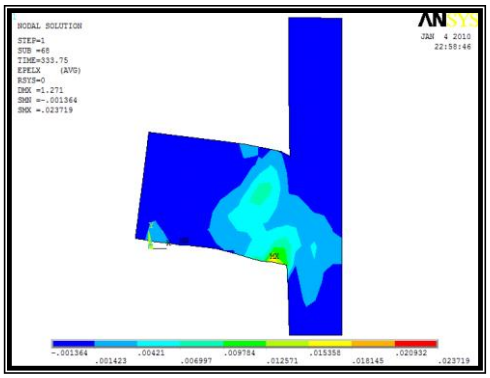

Fig. 27. Variation of strain in x-direction along quarter of concrete corbel CIS2 at ultimate load.

4.3. Strain in Concrete

The numerical concrete strains are obtained at the same positions where the corresponding experimental strains are recorded. A comparison between experimental and numerical concrete strain distribution shows good agreement within the elastic of behaviour or before cracking.

Table 4 shows the numerical and experimental compressive strains of concrete located at 20 mm from top and bottom face, and at column face of analyzed corbels. It may also be noted

that the numerical tensile strains of concrete are in good agreement with experimental data of corbels CONT1 and CIS2 at early stages of loading, while some difference between numerical and experimental strain occurred at final stages of loading. This difference is because that the presence of wide cracks at the tensile zone of mid span section.

Figs. 28 and 29 show a comparison between experimental and numerical concrete strain distribution for corbels CONT1 and CIS2 respectively.

Table 4. Experimental (Mohamad Ali and Attiya, 2012) and numerical extreme fiber concrete compressive and tensile strains of corbels CONT1 and CIS2.

	Load		**50 kN**	**100 kN**	**180 kN**	**270 kN**
CONT1	Num	Ten.	0.0008	0.0012	0.0018	0.0025
		Com.	-0.0005	-0.0006	-0.0009	-0.00157
	Exp.	Ten.	0.0006	0.0009	0.0016	0.00204
		Com.	-0.00035	-0.0008	-0.0013	-0.00192
	Load		**130 kN**	**220 kN**	**300 kN**	**380 kN**
CIS2	Num	Ten.	0.001	0.0014	0.0018	0.0023
		Com.	-0.0009	-0.00153	-0.00173	-0.00214
	Exp.	Ten.	0.0008	0.0009	0.0013	0.0015
		Com.	-0.0009	-0.00145	-0.0016	-0.00199

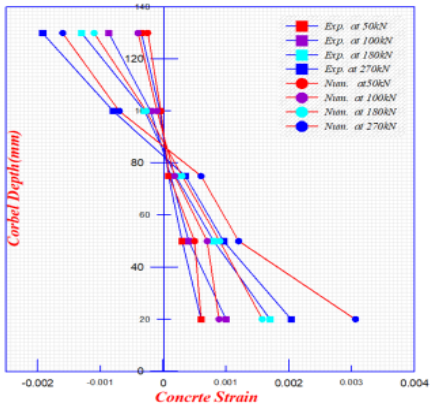

Fig. 28. Comparison between numerical and experimental (Mohamad Ali and Attiya, 2012) for concrete strain distribution for Corbel CON.

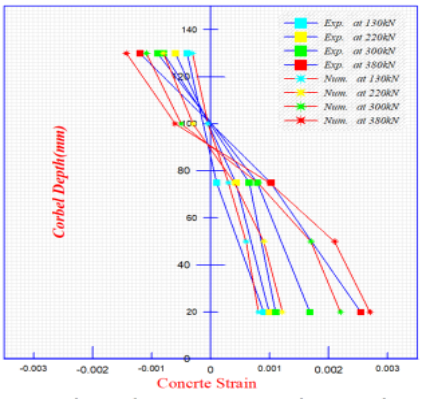

Fig. 29. Comparison between numerical and experimental (Mohamad Ali and Attiya, 2012) for concrete strain concrete distribution for Corbel CIS2.

Fig. 30. shows a comparison between numerical and experimental tensile strain developed in 1st and 2nd inclined strips of corbel CIS2, the development of tensile strains gives good agreement between numerical and experimental results.

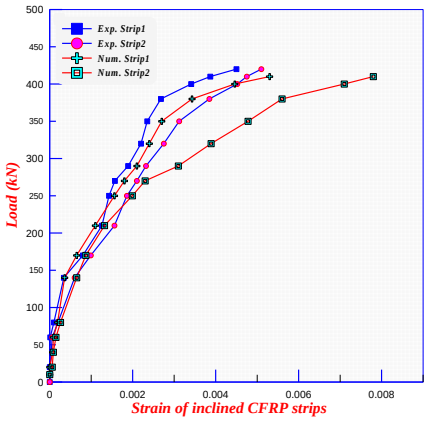

Fig. 30. Development of tensile strain in Inclined CFRP Strips of Corbel CIS2

4.5. Tensile Stress in CFRP

The finite element solutions reveal that the maximum stress developed in each CFRP strips is smaller than ultimate stress of CFRP strips which was 3500 MPa. Failure of the corbels occurred due to presence of diagonal shear cracks. These cracks occur at integration points of the solid brick elements. At ultimate load level, the CFRP strips ruptured at regions where the major diagonal shear cracks. Figs. 31 - 39 shows variation of tensile stresses developed in CFRP inclined strips at different loading stages for corbel specimens of series CIS and CISR.

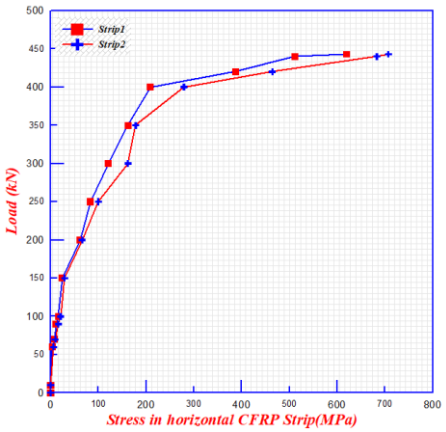

Fig. 31. Development of tensile stresses in Inclined CFRP Strips of Corbel CIS2.

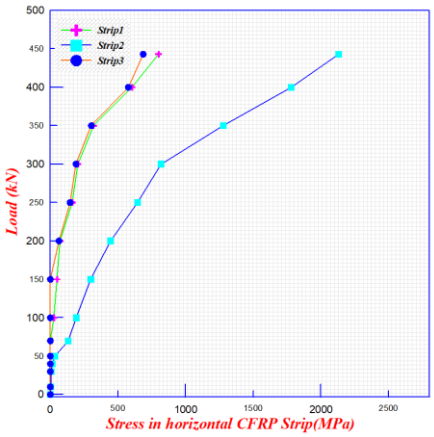

Fig. 32. Development of tensile stresses in Inclined CFRP Strips of Corbel CIS3

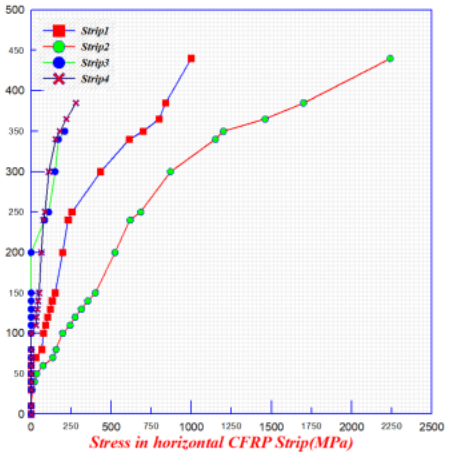

Fig. 33. Development of tensile stresses in Inclined CFRP Strips of Corbel CIS4

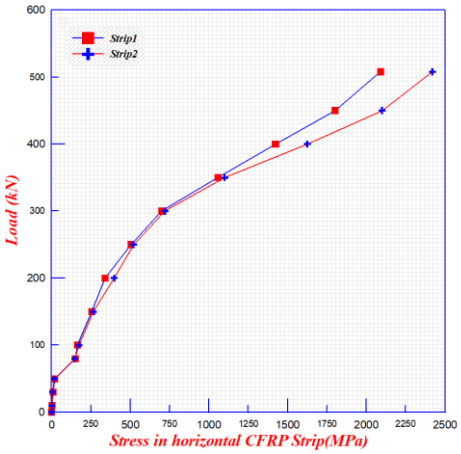

Fig. 34. Development of tensile stresses in Inclined CFRP Strips of Corbel CISR2

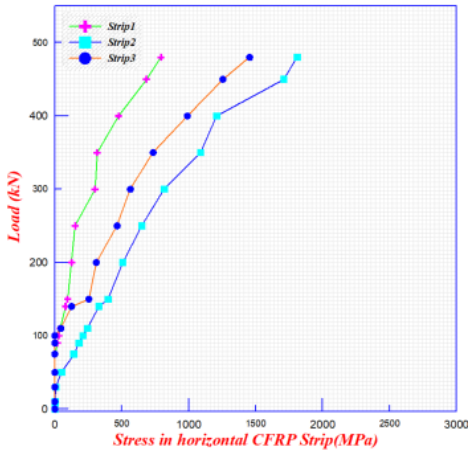

Fig. 35. Development of tensile stresses in Inclined CFRP Strips of Corbel CISR3

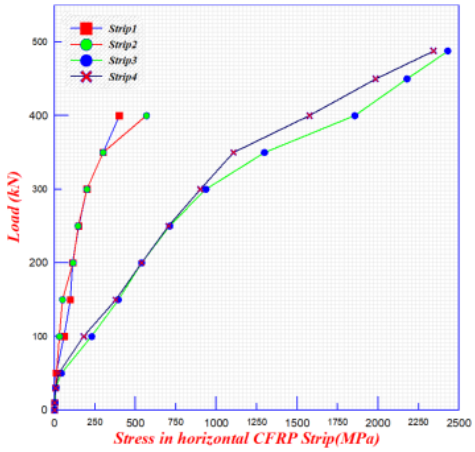

Fig. 36. Development of tensile stresses in Inclined CFRP Strips of Corbel CISR4

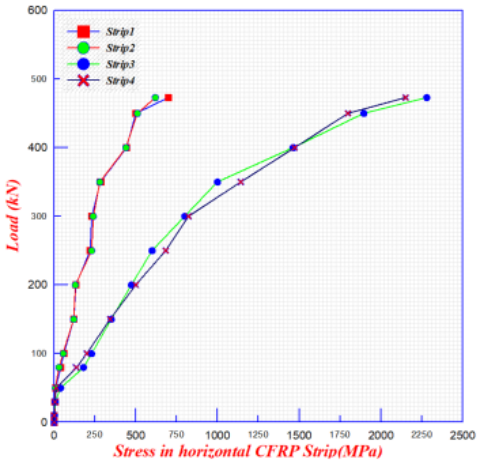

Fig. 37. Development of tensile stresses in Inclined CFRP Strips of Corbel CISFR4

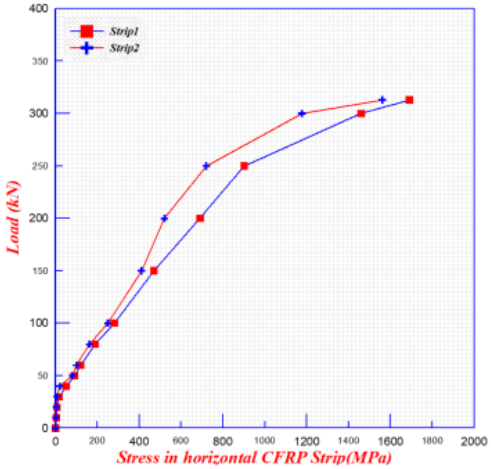

Fig. 38. Development of tensile stresses in Inclined CFRP Strips of Corbel CISR2 (a/d=1.0).

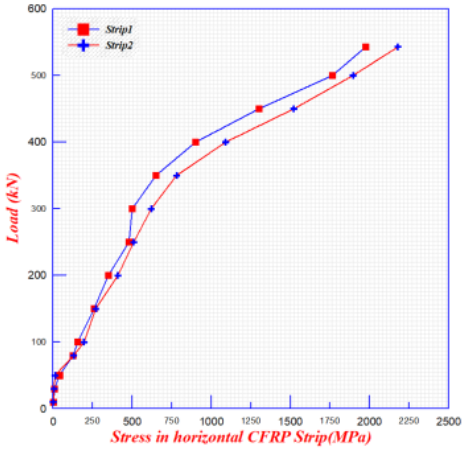

Fig. 39. Development of tensile stresses in Inclined CFRP Strips of Corbel CISR2 (a/d=0.5).

5. CONCLUSIONS

Based on the overall results obtained from the finite element analysis for the externally strengthened reinforced concrete corbels by CFRP strips, the following conclusions can be drawn:

1. The three-dimensional nonlinear finite element model adopted in the present research work is suitable for predicting the behaviour of the strengthened reinforced concrete corbel with CFRP sheets. The numerical results are in good agreement with experimental load-deflection results throughout the entire range of the behaviour. The maximum difference in the ultimate load was less than 10%.
2. The cracking patterns obtained from the finite element models are similar to the crack patterns observed in the experimental work, where all the analyzed corbels failed with a mode of failure similar to that which occurred in the experimental test.
3. The tensile strain in CFRP obtained from finite element analysis is in good agreement with those obtained from experimental work, especially at the early load stages.
4. The concrete strain at different stages of loading observed from the finite element model is in good agreement with those obtained from experimental work.
5. The finite element analysis reveals that the maximum tensile stresses developed in CFRP strips at failure ranged between (522) and (2430) MPa for inclined CFRP strips respectively.

6. REFERENCES

Mattock, A.H., Chen, K.C. and Soongswang, K., 1976, “The behavior of reinforced concrete corbels”. PCI Journal, 21(2), pp.52-77.

American Concrete Institute (ACI). (2008), “Building code requirements for structural concrete” ACI 318-08, American Concrete Institute, Detroit.

Mohamad Ali, A. A., and Attiya, M. A. (2012), “Experimental Behaviour of Reinforced Concrete Corbels Strengthened with Carbon Fiber Reinforced Polymer Strips”. Basrah Journal for Engineering Science, pp. 31–45

Bangash, M. Y. H., (1989), “Concrete and Concrete Structures: Numerical Modeling and Applications”, Elsevier Science Publishers, LTD., Essex, England.

Willam, K. J. and Warnke, E. P. (1975), “Constitutive Model for the Triaxial Behavior of Concrete”. Proceedings, International Association for Bridge and Structural Engineering, 19, ISMES, Bergamo, Italy, pp.174.

Al-Shaarbaf, I. A. S. (1990), "Three-Dimensional Non-Linear Finite Element Analysis of Reinforced Concrete Beams in Torsion" Ph.D. Thesis University of Bradford, U.K.

Sika, "Sika Warp®- 230C Woven carbon fiber fabric for structural strengthening", Technical Data Sheet, Edition 2, 2005.

ANSYS, 2007, "ANSYS Help," Release 11.0.